Evidence for rapid large-amplitude vertical motions in the Valencia Trough (Western Mediterranean) generated by 3D subduction slab roll-back

Penggao Fang, Julie Tugend, Geoffroy Mohn, Nick Kusznir, Weiwei Ding

Earth and Planetary Science Letters 575 (2021) 117179

Contents lists available at ScienceDirect

Earth and Planetary Science Letters

www.elsevier.com/locate/epsl

Evidence for rapid large-amplitude vertical motions in the Valencia Trough (Western Mediterranean) generated by 3D subduction slab roll-back

Penggao Fang [a,b], Julie Tugend [c,d,*], Geoffroy Mohn [d], Nick Kusznir [e], WeiWei Ding [a,b,**]

[a] Key Laboratory of Submarine Geosciences & Second Institute of Oceanography, Ministry of Natural Resources, Hangzhou 310012, China
[b] Southern Marine Science and Engineering Guangdong Laboratory, Zhuhai, 519082, China
[c] Sorbonne Université, CNRS-INSU, Institut des Sciences de la Terre de Paris, ISTeP UMR 7193, F-75005 Paris, France
[d] Géosciences et Environnement Cergy (GEC), CY Cergy Paris Université, Neuville-sur-Oise, 95000, France
[e] Department of Earth, Ocean and Ecological Sciences, University of Liverpool, Liverpool L693GP, UK

ARTICLE INFO

Article history:
Received 31 March 2021
Received in revised form 23 August 2021
Accepted 26 August 2021
Available online 27 September 2021
Editor: H. Thybo

Keywords:
Valencia Trough
Western Mediterranean
vertical movements
subduction dynamics
flexural backstripping

ABSTRACT

The mechanisms controlling the Cenozoic subsidence of the Valencia Trough, located in the Western Mediterranean, are poorly understood. The Cenozoic geodynamic evolution of the Western Mediterranean is complex comprising subduction, slab roll-back, back-arc extension, collision, and lithosphere delamination. We investigate the subsidence of a regionally observed unconformity, here referred to as the Miocene Unconformity, which separates Mesozoic from latest Palaeogene to Neogene sediments. Using a dense grid of seismic reflection data, well data and 3D flexural backstripping, we show that the Miocene Unconformity in the SW Valencia Trough subsided by more than 1.5 km to the present day at an average rate of 90 m/Myr. The absence of Cenozoic extensional faults affecting the basement shown by seismic data indicates that this rapid subsidence is not caused by Cenozoic rifting or remaining Mesozoic post-rift thermal subsidence. Neither can this subsidence be explained by subduction dynamic subsidence or flexural loading related to the thin-skin Betic fold and thrust belt which only affects subsidence observed near the deformation front.

We interpret the 1.5 km subsidence of the Miocene Unconformity as the collapse of a back-arc transient uplift event. Erosion during this uplift, resulting in the formation of the Miocene Unconformity, is estimated to exceed 4 km. Transient uplift was likely caused by heating of back-arc lithosphere and asthenosphere, combined with mantle dynamic uplift, both caused by segmentation of Tethyan subduction resulting in slab tear. Subsidence resulted from thermal equilibration and the removal of mantle flow dynamic support Tethyan subduction slab roll-back. We propose that our observations and interpretation of rapid back-arc km-scale uplift and collapse have global applicability for other back-arc regions experiencing subduction segmentation and slab tear during subduction slab roll-back.

1. Introduction

The formation of the Western Mediterranean in a subduction-related setting is controlled by the interaction of slab roll-back, back arc extension, collision, and lithosphere delamination processes. In such complex geodynamic context, it is often difficult to decipher the mechanisms which controls sedimentary basin subsidence history and distinguish the contribution of surface tectonics from dynamic topography.

The Valencia Trough is one of the main basins of the Western Mediterranean which formed in the late Oligocene to early Miocene in relation with the slab roll-back of the Tethyan oceanic lithosphere (Faccenna et al., 2004; Van Hinsbergen et al., 2014). It is bordered by the Iberian and Catalan Costal Ranges to the west, the Balearic fold and thrust belt to the east and the Betic orogenic system to the south (Fig. 1a). It is floored in its central part by thin continental crust with a shallow lithosphere asthenosphere boundary underneath (Watts and Torné, 1992a, 1992b; Ayala et al., 2015). Rift structures are observed in the north-eastern part of the Trough and are connected to the late Oligocene to early Miocene horst and graben system observed in the nearby Gulf of

* Corresponding author at: Géosciences et Environnement Cergy (GEC), CY Cergy Paris Université, Neuville-sur-Oise, 95000, France.
** Corresponding author at: Key Laboratory of Submarine Geosciences & Second Institute of Oceanography, Ministry of Natural Resources, Hangzhou 310012, China.
E-mail addresses: julie.tugend@gmail.com (J. Tugend), wwding@sio.org.cn (W. Ding).

https://doi.org/10.1016/j.epsl.2021.117179

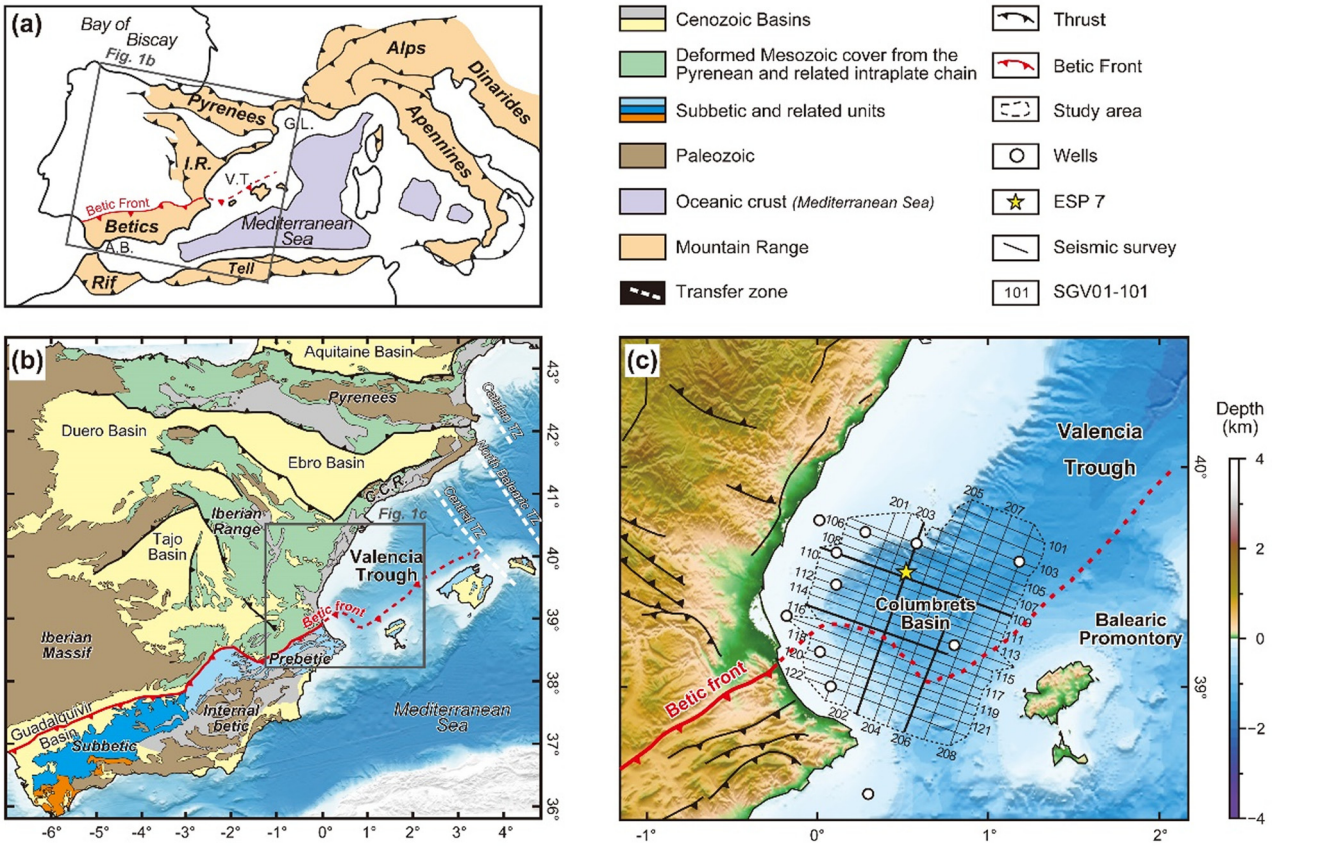

Fig. 1. (a) Map of the western Mediterranean region showing the location of the Valencia Trough in the frame of the Alpine and Betic orogenic belts (modified after Roca, 2001). (b) Tectonic map of eastern Iberian Peninsula and the Valencia Trough. (c) Enlarged map showing the location of the data sets used in this study (SGV seismic survey, wells and ESP data). A.B.: Alboran Basin; C.B.: Columbrets Basin; C.R.R.: Catalan Coastal Range; G.L.: Gulf of Lion; I.R.: Iberian Range.

Lion (Maillard and Mauffret, 1999; Roca, 2001). However, in the south-western part of the Valencia Trough evidence of this rifting is sparse or absent (Fig. 1b, Roca and Guimerà, 1992). Also, the southern and south-western parts of the Valencia Trough are largely affected by the propagation of the Betic fold and thrust belt during the early to middle Miocene.

Successions younger than the Oligocene recording these different tectonic events are delimited from the underlying ones by a major unconformity observed throughout the Valencia Trough (e.g., Maillard et al., 1992) and here referred to as the Miocene Unconformity. The geodynamic significance of this regional unconformity, the amplitude of associated vertical movements and mechanisms controlling the subsidence evolution of the Valencia Trough during the early Cenozoic are poorly understood.

Here we use a dense grid of seismic reflection data, well data and 3D flexural backstripping to investigate the formation processes and subsidence evolution of this Miocene Unconformity. Previous works focused on rift-related subsidence mechanisms or flexural loading effects (Roca and Desegaulx, 1992; Watts and Torné, 1992b; Torres et al., 1993; Janssen et al., 1993). In contrast, our analysis suggests that the formation and present-day subsidence of the Miocene Unconformity is best explained by the collapse of mantle dynamic uplift combined with lithosphere thermal re-equilibration after segmentation and slab tear in the Tethyan subduction. Flexural loading effects exist but only in the immediate vicinity of the Betic fold and thrust belt.

2. Tectono-stratigraphic context

The stratigraphic framework of the Valencia Trough is reasonably well constrained thanks to decades of exploration (e.g., Maillard et al., 1992; Roca and Guimerà, 1992; Granado et al., 2016; Cameselle and Urgeles, 2017; Etheve et al., 2018; Roma et al., 2018). A coherent seismic stratigraphy of the south-western Valencia Trough has recently been proposed based on the same dataset as the one used in this study which includes the oldest Mesozoic sequences (Fig. 2, Etheve et al., 2018). The identification of different seismic units is based on the recognition of major unconformities in reflection seismic profiles calibrated from drill core observations where possible (Fig. 3) and onshore field analogies as well as seismic facies variations combined to P-wave velocity information (e.g., Watts and Torné, 1992b). These different seismo-stratigraphic units are then assimilated to sedimentary sequences deposited during the different tectonic events which affected Eastern Iberia and described hereafter.

The oldest sediments evidenced in the region of the Valencia Trough are Permo-Carboniferous to Middle Triassic in age and assimilated as part of the “acoustic basement” (Fig. 2, Seismic Unit – SU G, Etheve et al., 2018). This sequence includes continental siliciclastic sediments deposited at the end of the Variscan orogeny and during Late Permian to Early Triassic intra-continental rifting (Arche and López Gómez, 1996). They are replaced upsection by post-rift shallow marine carbonates and minor evaporite interbeds of Middle Triassic age (Alba, 2007).

Renewed extension occurred during the Late Triassic to Middle Jurassic period related to Alpine Ligurian Tethys opening further to the east. During this period thick Upper Triassic evaporites were deposited, dominated by anhydrite and halite with terrigenous and dolostone interbeds (SU F, Ortí et al., 2017). On top, a shallow marine platform developed in latest Triassic time grading into limestones and marls during the Sinemurian to Middle Jurassic (SU E, Roca, 1996).

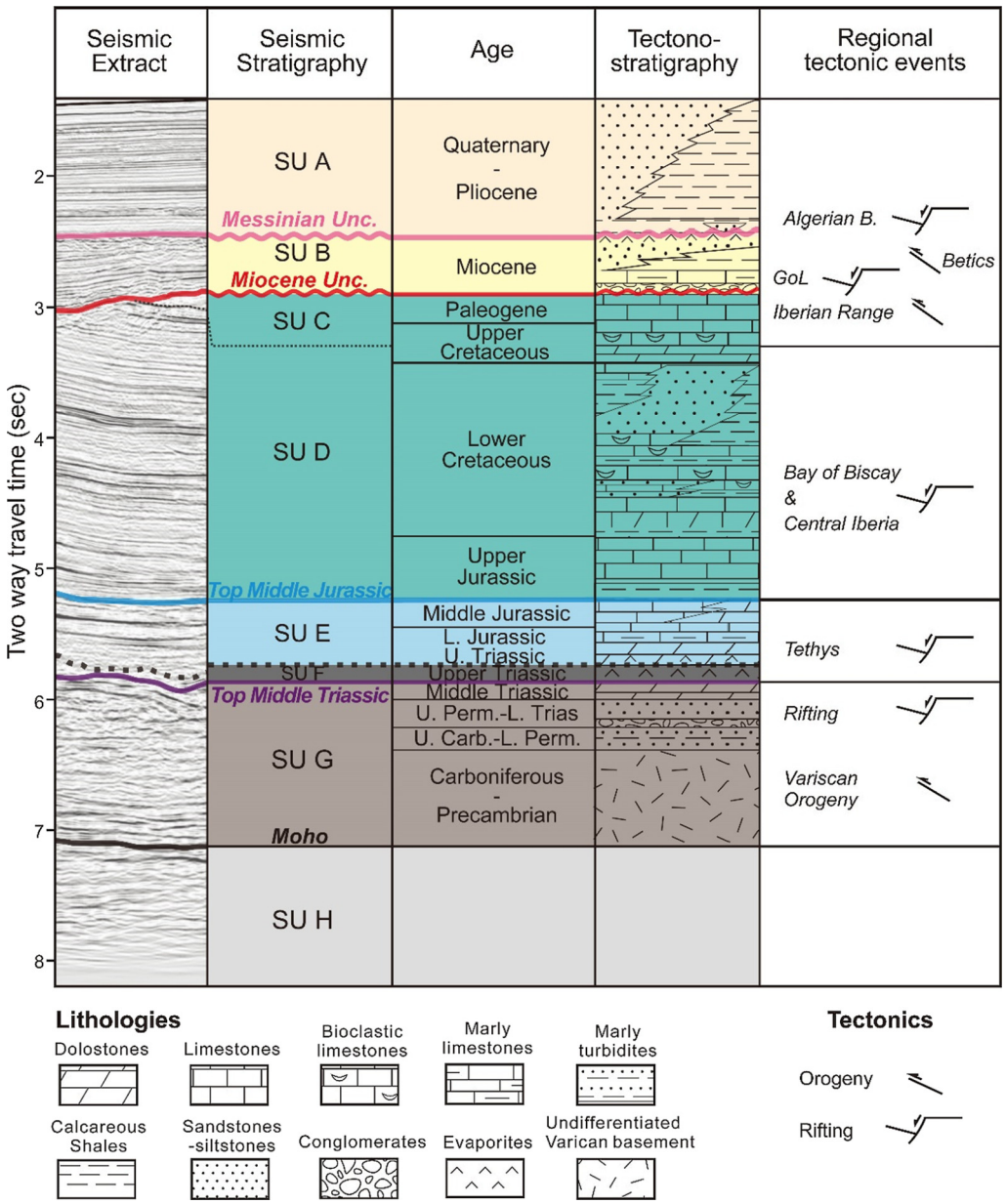

Fig. 2. Seismic stratigraphy, inferred age and lithologies of the main sedimentary units deposited in the SW Valencia Trough (modified after Etheve et al., 2018). Related regional tectonic events which affected the south-western part of the Valencia Trough are also indicated. Seismic data is extracted from the SGV01-109 profile (see Fig. 1 for its location).

Late Jurassic to Early Cretaceous sediments (SU D, Etheve et al., 2018) were deposited during the main rifting phase which resulted in the extreme thinning of the Columbrets basin (Roca, 1996; Etheve et al., 2018). The Columbrets Basin represents the eastern prolongation of the Central Iberian Rift system, the latter was subsequently inverted during the Paleogene and is now sampled in the Iberian Range (Fig. 1, Salas et al., 2001). At a larger scale, this rifting phase preceded the opening of Bay of Biscay oceanic basin to the west and is recorded in a series of basins scattered at the Iberian-European plate boundary (Tugend et al., 2015b). Oxfordian to Albian syn-rift successions show significant thickness variations with platform carbonates grading basinward into marls and local fluvial to deltaic interbeds of Barremian age near the basin margins (Fig. 2 and 3). Post-rift subsidence is recorded by late Albian sandstones and Cenomanian to Turonian dolostones (Etheve et al., 2018).

The overlying sequence (SU C) is only locally preserved. The top corresponds to a marked erosional unconformity which is regionally observed in the Valencia Trough (e.g., Maillard et al., 1992; Roca, 1996; Etheve et al., 2018; Roma et al., 2018). Since the first overlying sediments we observe in the south-western Valencia Trough are early Miocene (Aquitanian to Tortonian, Fig. 3), it is referred to in this work as the "Miocene Unconformity". The age of the underlying sequences as constrained by wells is variable ranging from Upper Triassic to Santonian (Fig. 3) depending on erosion intensity and on the structure of the Mesozoic Columbrets Basin. In our study area Palaeogene sequences of SU C were not recorded in wells (Fig. 3). Nevertheless, the local presence of Uppermost Cretaceous to Eocene successions is likely and consistent with the local occurrence of reworked Palaeogene faunas in the early Miocene sediments deposited on top of the unconformity (Fig. 3). Palaeogene sediments are, however, evidenced in wells in the NE Valencia Trough (e.g., Barcelona Basin) and consist of alluvial and lacustrine succession with marine incursions (Roca et al., 1999). Sediments of seismic unit C, where observed, were deposited during the convergence between Europe Iberia and

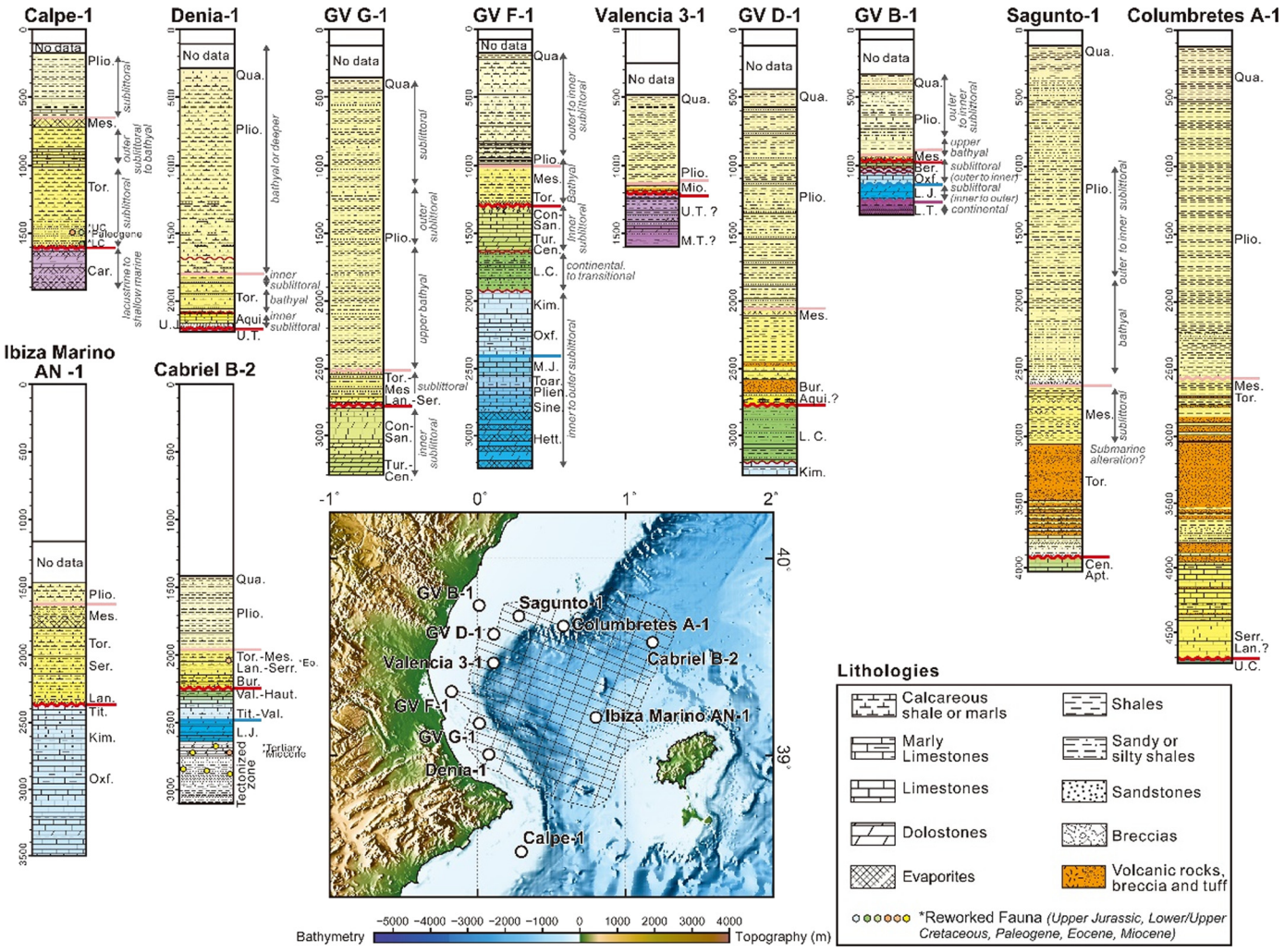

Fig. 3. Lithology, age and thicknesses of selected wells located in the SW Valencia Trough (after Lanaja, 1987). GV B-1: Golfo Valencia B-1; GV D-1: Golfo Valencia D-1; GV F-1: Golfo Valencia F-1; GV G-1: Golfo Valencia G-1. Qua.: Quaternary; Plio.: Pliocene; Mes.: Messinian; Tor. Tortonian; Lan.: Langhian; Serr.: Serravalian; Bur.: Burdigalian; Aqui.: Aquitanian; San.: Santonian; Con.: Coniacian; Tur.: Turonian; Cen.: Cenomanian; U.C.: Upper Cretaceous; Apt.: Aptian; Haut.: Hauterivian; Val.: Valanginian; Berr.: Berriasian; L.C.: Lower Cretaceous; Tit.: Titonian; Kim: Kimeridgian; Oxf.: Oxfordian; M.J.: Middle Jurassic; Toar.: Toartian; Plien: Pliensbachian; Sin.: Sinemurian; Hett.: Hettangian; L.J.: Lower Jurassic; Car.: Carnian; U.T.: Upper Triassic; M.T.: Middle Triassic; L.T.: Lower Triassic.

Africa, which started in the Late Cretaceous. Early Palaeogene sequences recorded the inversion of former Mesozoic rift basins and building of intracontinental mountain belts in the Iberian Range to the west (Guimerà Rosso, 2018), Pyrenees to the north (Tugend et al., 2015b) and Betics to the south (Platt et al., 2013). Related deformation is also observed in the Valencia Trough but is less intense (Klimowitz et al., 2018; Roma et al., 2018).

The first sediments deposited on top of the Miocene Unconformity are Aquitanian to Langhian where drilling controls are available (Fig. 3). They consist of detrital conglomerates and sandstones grading upsection to marine platform carbonates and marls while the overlying Serravallian to Messinian sequence includes terrigenous progradational deposits (SU B, Roca et al., 1999). Sediments of unit B were deposited during the rifting and opening of the Liguro-Provençal basin in relation with the south-westward and south-eastward retreat of the subducted Tethys (Faccenna et al., 2004; Van Hinsbergen et al., 2014). The record of this extensional deformation differs between the north-east and south-western parts of the Valencia Trough. In the north-east, onset of extension is late Oligocene (~28 Ma) related to the formation of a series of half grabens onshore and offshore Barcelona (Roca et al., 1999). In the south-west, only sparse structures are identified, and extensional deformation is delayed to the early Miocene age (~22 Ma) (e.g., Etheve et al., 2016). During the early to middle Miocene, the southern edge of the Valencia Trough was affected by the Betic fold and thrust belt (Roca et al., 2006; Etheve et al., 2016). This deformation is characterized by a strong decoupling along Upper Triassic evaporites between the para-autochthonous Jurassic to Miocene cover and autochthonous Iberian basement (Roca et al., 2006). The deformation front, referred to as the Betic Front, can be followed from the Iberia Peninsula to the Balearic Promontory (Fig. 1c).

The overlying sediments of SU A consist of a terrigenous shelf-talus system including sandstones, shales and marls prograding on top of the so-called Messinian unconformity (Maillard et al., 2006). They record a diffuse extension initiated in the middle Miocene in relation with the evolution of the Algerian Basin further to the east (Sàbat et al., 1997).

3. Analysis of seismic and well data

3.1. Multichannel seismic reflection data and expanded spread data

We analysed and interpreted 30 multichannel reflection seismic profiles (~2800 km) located in the SE part of the Valencia Trough (Fig. 1b). The 2D multichannel reflection seismic survey includes profiles arranged in WNW-ESE and NNE-SSW directions with a

maximum separation of 13 km and 6 km respectively (Cameselle and Urgeles, 2017). It was acquired by Fugro-Geoteam aboard the *R/V Geo Baltic* in October 2001. Detailed acquisition parameters and processing work are presented in Cameselle and Urgeles (2017) (see Table A.1). The seismic interpretation work was undertaken in two-way travel time (s, TWT) using the Petrel software.

A series of 6 Expanded Spread Profiles (ESP) were acquired by the *N/O Jean Charcot* and *R/V Robert D. Conrad* in 1988 in the Valencia Trough (see detailed acquisition configuration and processing in Pascal et al., 1992; Torné et al., 1992). During this two-ship experiment, multiple-fold wide-angle reflection/refraction data sets were acquired, one ship acted as the seismic source (*R/V Robert D. Conrad*) while the other was recording (*N/O Jean Charcot*). In this study, we used the results presented by Torné et al. (1992) and Pascal et al. (1992) for the ESP 7, located in the SW part of the Valencia Trough in the Columbrets basin (Fig. 1c).

3.2. Well data

Our seismic stratigraphy is calibrated from a total of 11 exploratory wells (Fig. 3, Lanaja, 1987). The correlation between seismostratigraphic interpretations and geological constraints was a prerequisite to infer ages and depositional environment of the different tectono-sedimentary units (Fig. 2). Most of the wells are located on the present-day shelf (Fig. 3, CALPE-1, DENIA-1, GV G-1, GV F-1, GV D-1, GV B-1, COLUMBRETES A-1, and SAGUNTO-1), one is located on the upper slope (VALENCIA 3-1), two are located in the deep basin (IBIZA MARINO AN-1 and CABRIEL B-2). All these wells demonstrate the absence of Palaeogene sequences (Fig. 3). Only reworked Palaeogene faunas are locally recovered in the first Miocene sediments directly overlying eroded Mesozoic sequences (Fig. 3, CALPE-1 and CABRIEL B-2). This absence marks a remarkable unconformity described regionally directly overlain by early Miocene sediments and corresponding to the "Miocene unconformity" (Maillard et al., 1992; Sàbat et al., 2011; Etheve et al., 2018).

3.3. Depth conversion

We applied a constant velocity of 1.524 km.s^{-1} to the water column. We determined a depth conversion law from the velocity information provided by the ESP 7 (Fig. 2, Pascal et al., 1992; Torné et al., 1992), which we applied to the Messinian and Miocene unconformities as well as to the Top Middle Jurassic horizon grids interpreted in two-way travel time (s, TWT). This law is calibrated from velocity data points of the ESP 7 for which both the depth (km) and TWT (s) could be determined. The resulting time-depth relationship is satisfied by a second order polynomial trend curve (see Figure A.1). The depth to the Top Middle Triassic/Top of "acoustic basement" horizon is determined by applying a constant velocity of 6.6 km.s^{-1} to the seismic units E and F (Fig. 2), mostly corresponding to carbonates and evaporites of Upper Triassic age according to drilling results (Fig. 3). A constant velocity of 6.8 km.s^{-1} is applied to the Paleozoic basement (seismic unit G) to depth convert the Moho interpreted by Etheve et al. (2018) for the crustal scale representation in Fig. 4. We tested our depth conversion against drilling results and the results show a good correlation (Fig. 4b).

3.4. Structural and stratigraphic architecture of the SW Valencia Trough from seismic interpretation

We have investigated stratigraphic relationships and mapped the main structures observed in the south-western part of the Valencia Trough from reflection seismic profiles (Fig. 5, 6 and 7). The depth conversion of the different identified horizons (Fig. 2, Figure A.2) enabled us to compile sedimentary thickness maps and to investigate the main tectonic structures which may have controlled the distribution of the first sediments directly overlying the Miocene Unconformity (Fig. 7e). The distribution of the sedimentary unit B is not homogeneous across the study area (Fig. 7b) and two main structural domains can be distinguished delimited by the Betic front (Fig. 5, 6 and 7).

Directly north of the Betic front, thick Miocene sediments of unit B (locally more than 1.5 km thick) were deposited (Fig. 7b) and passively onlapped the underlying eroded Mesozoic (and possibly Palaeogene) sediments (Fig. 5b, Fig. 6d). The Miocene Unconformity corresponds to a rough surface (Fig. 7e), which is usually not controlled by Cenozoic faulting but instead by the underlying faulted Mesozoic sequence as shown by reflection seismic data (Fig. 5d&e, Fig. 7d). We identified only a few normal faults which affect the earliest Miocene sediments most of them being localized on top of underlying Mesozoic faults (e.g., Fig. 5b, near the intersection with line 206, Fig. 7e). Younger faults are observed and control the deposition of latest Miocene to Pliocene sediments (Fig. 7a&e) as shown by well developed growth strata, the most striking one being known as the Valencia fault (Fig. 5b&c, Fig. 7, Maillard and Mauffret, 2013). Our high resolution seismic data enables us to unambiguously show the listric geometry of the Valencia Fault, detached on the Upper Triassic evaporite sequence acting as a major décollement. Previous works using lower resolution seismic data considered this fault as part of the Oligocene to earliest Miocene rift system (Maillard and Mauffret, 2013) which is observed further to the north-east of the Valencia Trough (e.g., Barcelona graben, Roca et al., 1999). Even though an early Miocene activation is likely, our observations suggest that this fault was mainly active during the latest Miocene to Pliocene.

Our dense and high resolution seismic observations confirm the lack of extensional structures formed during the Oligo-Miocene rifting in the south-western Valencia Trough in contrast to observations made further to the north-east (Maillard et al., 1992; Roca et al., 1999) and in the Gulf of Lion (Gorini et al., 1993). Thick Miocene sequences are also observed in the northern part of our study area. There, Neogene volcanics and sediments up to 2 km thick are observed in the Columbrets A-1 well and decrease to ~1.5 km in the western Sagunto A-1 well (Fig. 3). The northward thickening of unit B should be interpreted with caution but could partly correspond to increasing Neogene volcanics mapped as part of the sediments of unit B (Fig. 5 and 6) related to the activity of the northern Columbrets Island volcanic system (Maillard et al., 1992). The occurrence of these Neogene volcanic sequences creates uncertainties on the seismic interpretation and depth conversion of sequences older than Pliocene.

South of the Betic front, the main depocentres of Miocene sediments (up to 1.5 km thick) show ellipsoid patterns. There, the depth to the Miocene Unconformity also corresponds to a rough surface showing high amplitude variations (Fig. 7e), controlled by the salt-influenced thin-skinned deformation style of the most external part of the Betic fold and thrust belt (Fig. 6). There, several unconformities are often observed in Neogene sediments (e.g., DENIA-1, Fig. 3) and the mapping of the Miocene Unconformity is locally related to uncertainties in the absence of direct well calibrations. These unconformities formed during the observed intense salt tectonic activity also documented in the adjacent onshore eastern Prebetics (e.g., Roca et al., 2006). The structural style is characterized by a succession of shortened salt structures where folds and thrusts nucleate, separated by synclines filled by Neogene sediments (Fig. 6). Along the profiles several common structures are recognized such as teardrop diapirs, diapir reactivated as a thrust (Fig. 6) suggesting that pre-existing salt structures were reactivated and confirming the long-lasting salt tectonic activity in this area. The amount of shortening is variable: only weakly reactivated salt

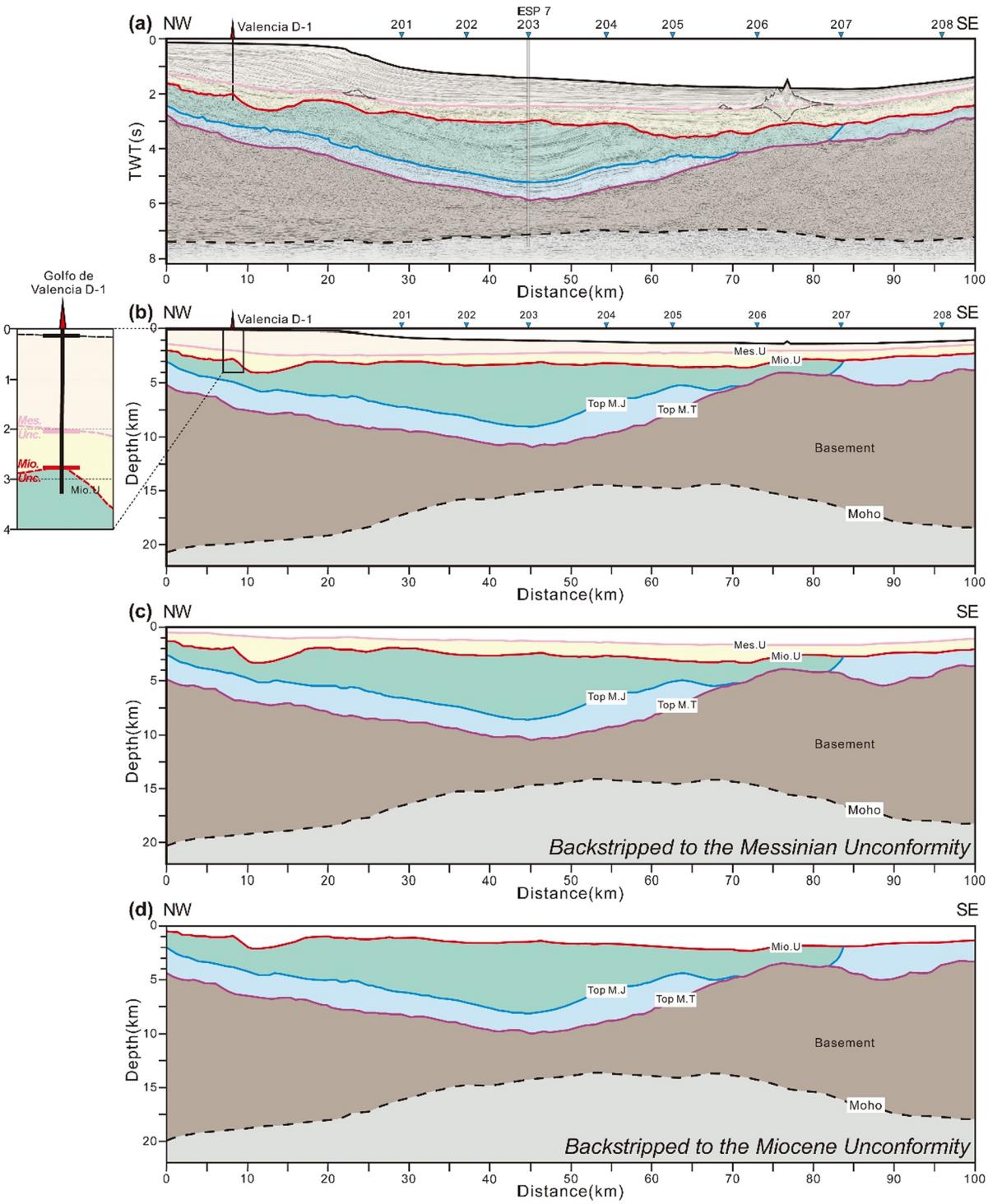

Fig. 4. (a) Interpreted SGV-01 109 reflection seismic profile (s, TWT) (after Etheve et al., 2018, see location in Fig. 1). (b) Depth conversion applied to the interpreted horizons of the SGV-01 109 profile. Note the good the correlation with the drilled results of the Golfo the Valencia D-1 well. (c) 2D flexural backstripping restored at the Messinian unconformity and (d) at the Miocene unconformity.

structures are observed to the west (Fig. 6a) whereas more intense deformation is evidenced further to the east showing squeezed diapirs (Fig. 6b).

The Betic front is often difficult to identify unambiguously and is mapped at the northern termination of reactivated former salt structures. North of it, Neogene sequences are sub-horizontal overlying the main depocenter of the Mesozoic Columbrets basin. The localization of the Betic Front and propagation of the Betic fold and thrust belt was likely controlled by the distribution of former Triassic evaporites prior to the Neogene. Such complex tectonic setting, with significant salt thickness variations and where salt mobility is expected may partly explain the contrasted deformation style of the external fold and thrust belt of the Betics (Fig. 6). The thin-skin deformation style of this external part of the Betic fold and thrust belt contrasts with the thick skin deformation suggested in the Balearic Promontory where the Upper Triassic salt layer is thinner (Fontboté et al., 1990; Sàbat et al., 2011; Etheve et al., 2016).

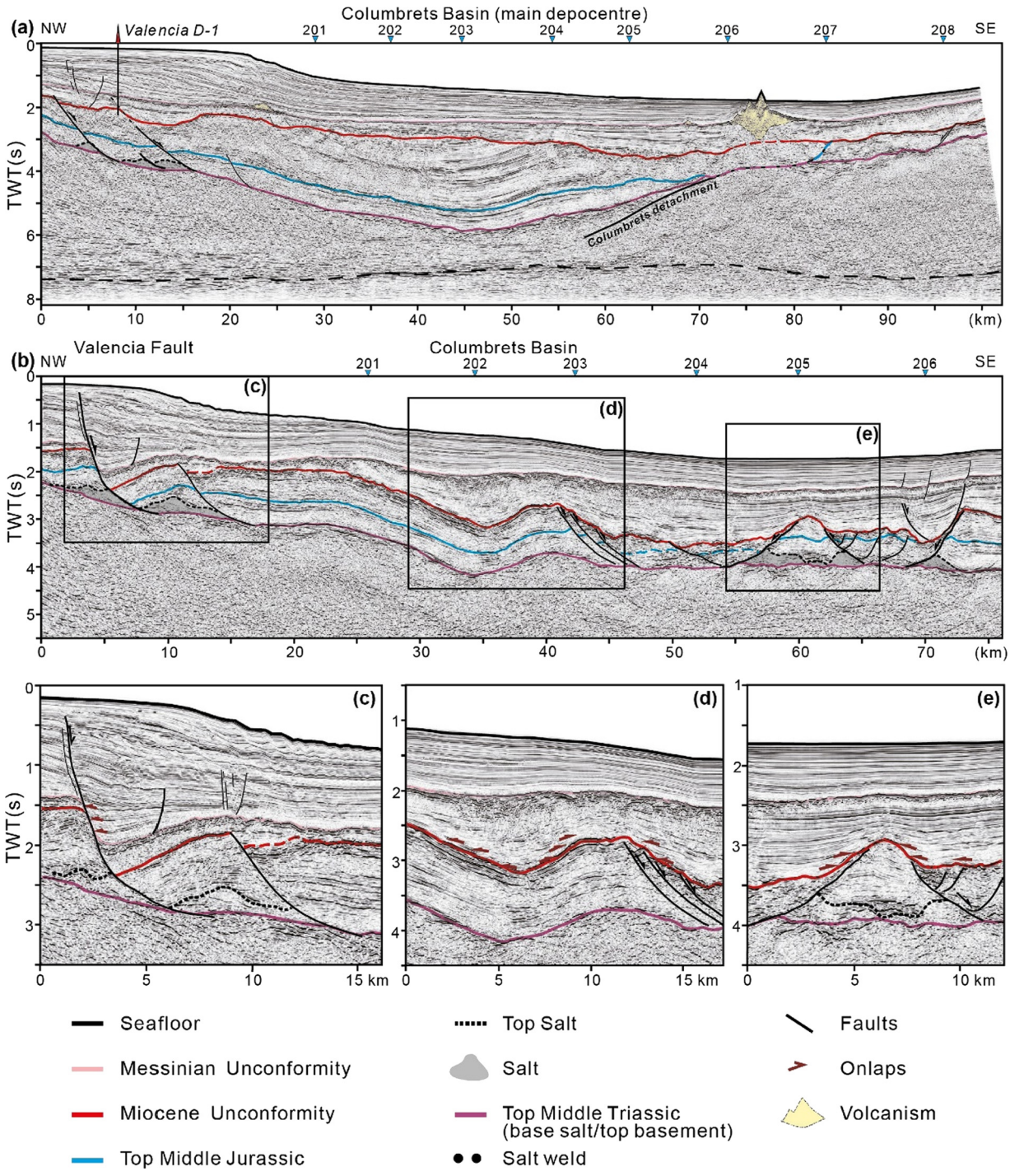

Fig. 5. Interpretation of the (a) SGV01-109 and (b) SGV01-115 NW-SE trending reflection seismic profiles (see location in Fig. 1). Interpreted zooms of the SGV01-115 profile over the structure of the (c) Valencia Fault, (d) southern Columbrets Basin and (e) Mesozoic salt-related rafts.

4. Subsidence analysis

4.1. Methodology using 3D flexural-backstripping

The Cenozoic subsidence evolution of the Valencia Trough has previously been investigated using 1D and 2D backstripping methods (Roca and Desegaulx, 1992; Roca and Guimerà, 1992; Watts and Torné, 1992b; Torres et al., 1993; Yamasaki and Stephenson, 2009). In this study, we use a 3D flexural-backstripping method to determine the subsidence of the Miocene Unconformity. We use 3D flexural backstripping to determine the bathymetry of the Miocene unconformity corrected for the loading of sediments above it. Removal of this sediment load results in isostatic rebound and partial decompaction of the remaining sediments. Both of these effects are calculated in the flexural backstripping procedure. Sediment decompaction is controlled by lithological parameters (Sclater and Christie, 1980), which we have determined from the drilling results (Fig. 3, Table A.2). We include all the sequences down to top basement in the decompaction.

4.2. Results of subsidence analysis

3D flexural backstripping and decompaction to remove sedimentary layers and loading above the Miocene Unconformity

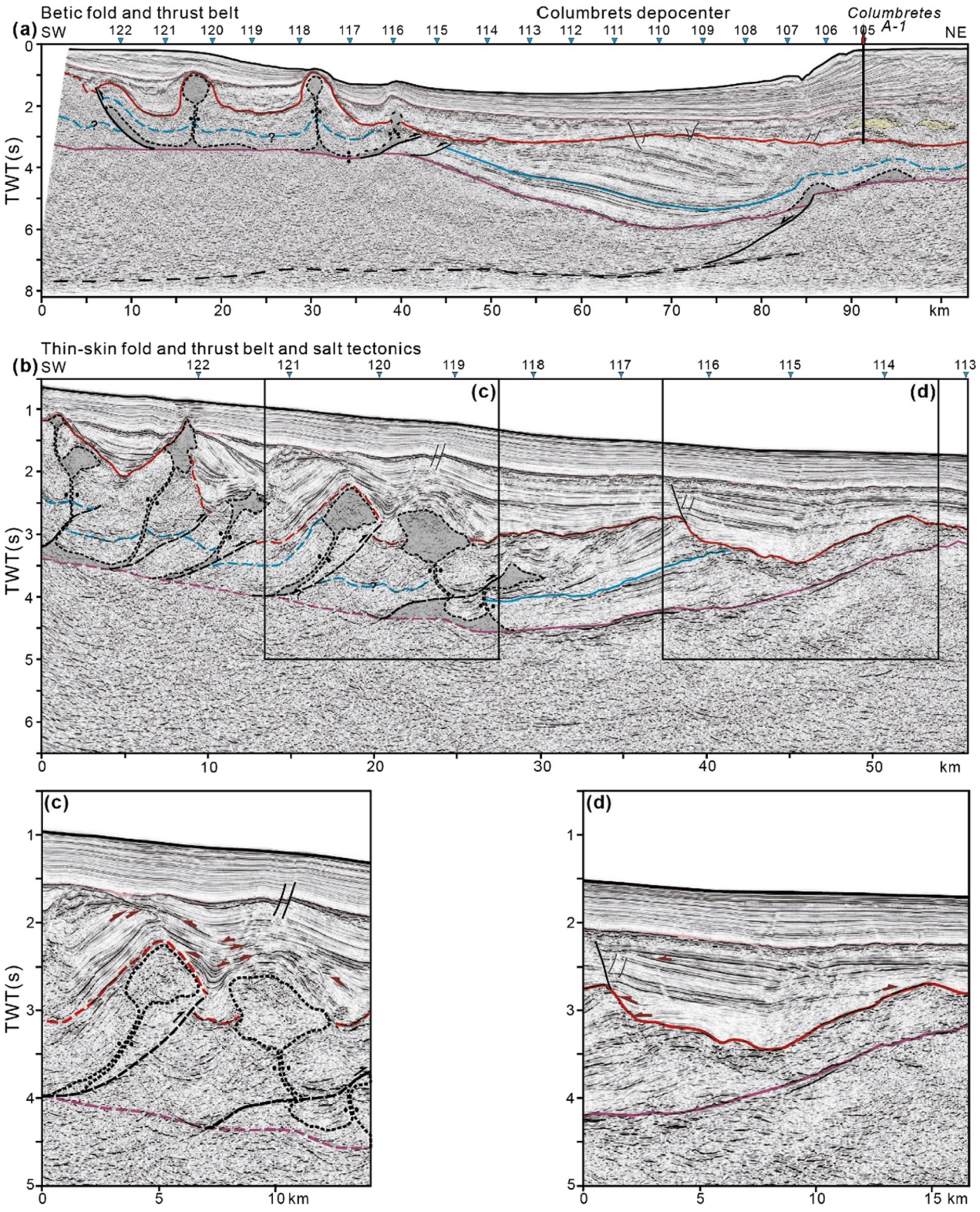

Fig. 6. Interpretation of the (a) SGV01-203 and (b) SGV01-206 NE-SW trending reflection seismic profiles (see location in Fig. 1). Interpreted zooms of the SGV01-206 profile over the structure of the (c) Betic fold-and-thrust belt and (d) related Miocene depocentre.

(Fig. 8a) gives sediment-corrected bathymetries shown in Figs. 8c-f. Drill core (Fig. 3) and seismic observations (Fig. 5 and 6) show that the Miocene Unconformity formed by erosion above or at sea level, in which case, the sediment-corrected bathymetry determined from backstripping represents the water-loaded subsidence of the Miocene unconformity.

Backstripping results are sensitive to the effective elastic thickness (Te), which we use to parametrize the effect of the flexural strength of the lithosphere (Fig. 8). The importance and sensitivity to Te in backstripping is discussed in Roberts et al. (1998). Backstripping results show very similar trends for the different tested values of Te (3, 5, 10 km, Fig. 8b) with the largest dif-

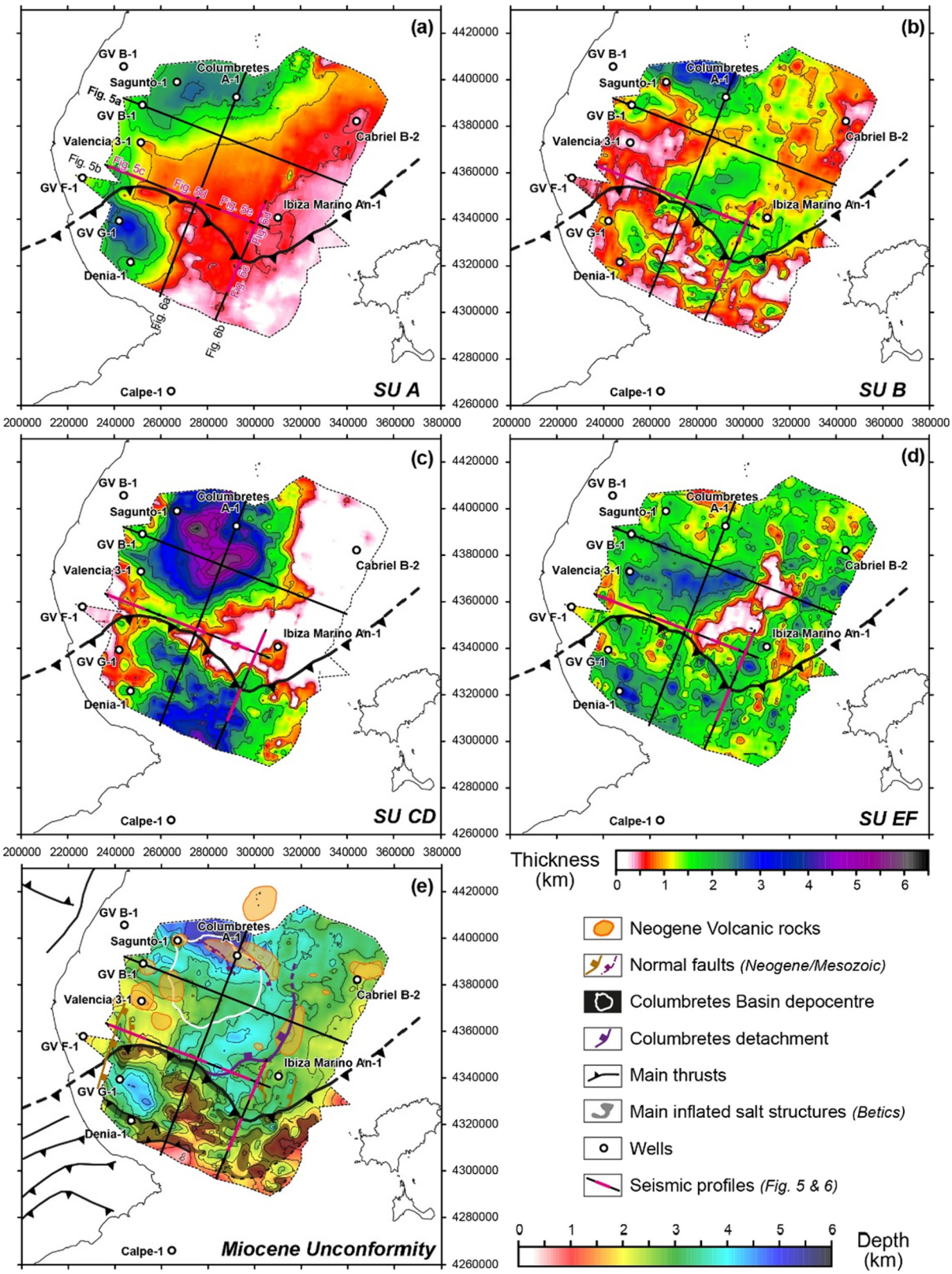

Fig. 7. Thickness maps of (a) Pliocene-Quaternary sediments (Seismic Unit A), (b) Miocene sediments (Seismic Unit B), (c) Upper Jurassic to Paleogene sediments (Seismic Units CD), (d) Middle Triassic to Middle Jurassic sediments (Seismic Units EF) (d) Structural map superimposed on the depth to the Miocene Unconformity. The Betic front as mapped in this work is indicated on all maps. Contours are given every 500 m.

ference being seen for Te=0 (Fig. 8c) which corresponds to airy local isostasy. Backstripping results converge for low Te values (Te $\leq$ 10), a result consistent with previous studies in the Valencia Trough (Janssen et al., 1993; Gaspar-Escribano et al., 2003) and adjacent Betic Cordilleras (Van der Beek and Cloetingh, 1992). The flexural rigidity of the lithosphere, however, increases under the Ebro Basin towards the Pyrenees (Gaspar-Escribano et al., 2001).

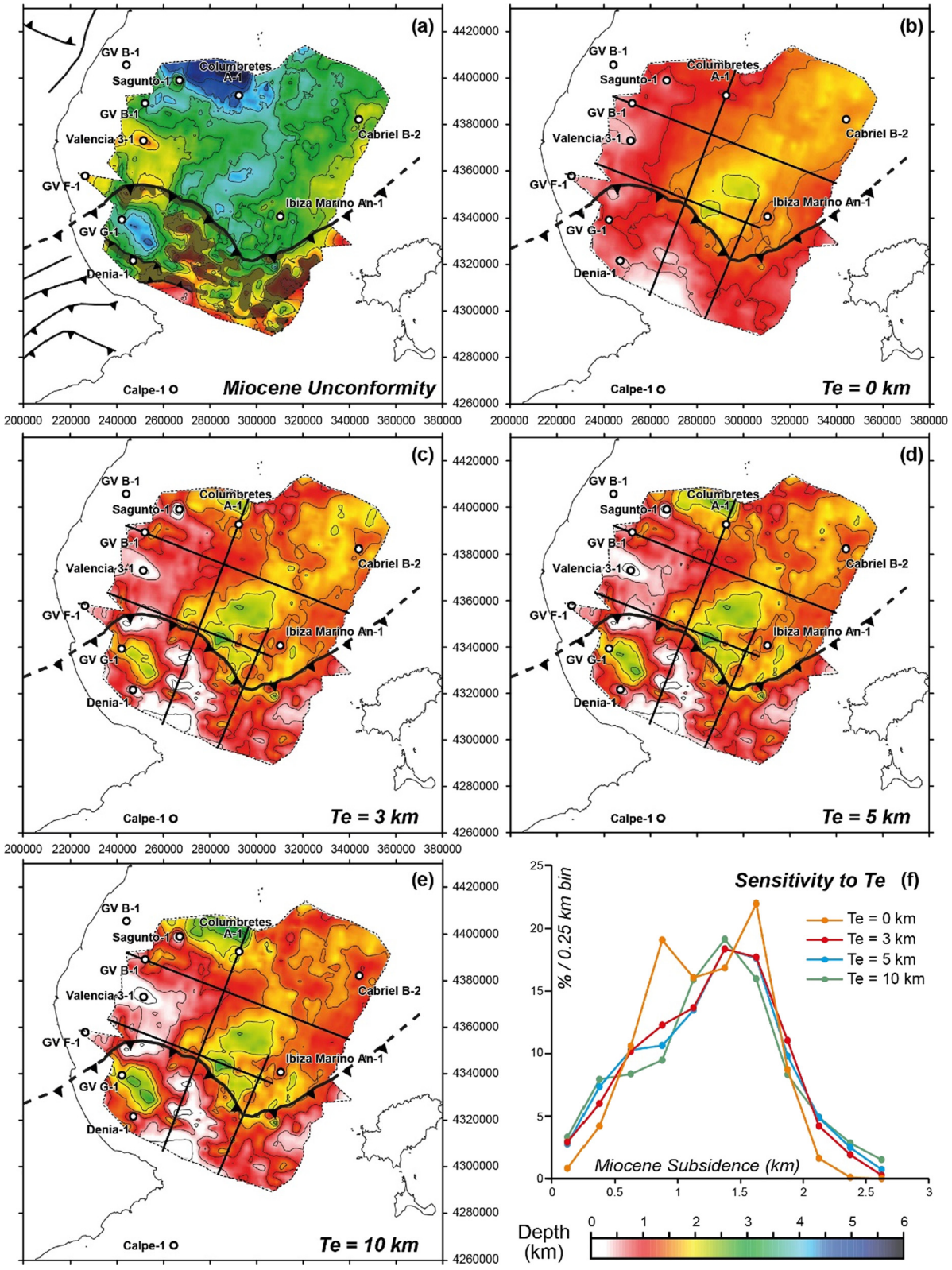

Fig. 8. (a) Map of the depth to the Miocene Unconformity (b-e) Backstripped maps at the Miocene Unconformity for an effective elastic thickness of (b) 0 km, (b) 3 km, 5 km and 10 km. The location of the Betic front is indicated on all maps. Contours are shown every 500 m. (f) Histograms showing the distribution of the Miocene subsidence for the different investigated values of Te.

The backstripped maps to the Miocene Unconformity show the heterogenous distribution of water-loaded subsidence across the study area. In order to evaluate Miocene water-loaded subsidence values at the regional scale we have made normalised histograms with 250 m subsidence intervals for each Te value (Fig. 8f). For Te $\geq$ 3, the histograms peak at just less than 1.5 km subsidence (Fig. 8f). 10% are shallower than 0.375 km for Te $\geq$ 3; these values are typically observed to the west of the study area and south of

the Betic front. Approximately 50% of our study area show values of water-loaded subsidence between 1.125 and 1.625 km. These values are typically observed north of the Betic front near the centre of the Valencia Trough and define an overall NE-SW trend. Values of water-loaded subsidence exceeding 2 km represent between 6 to 9% of the maps for Te $\geq$ 3 and are observed directly north of the Betic front and in the northernmost part of our study area. South of the Betic front, these large values of water-loaded subsidence define ellipsoid patterns (Fig. 8).

The decompaction procedure detailed above assumes that the lithologies beneath the Miocene Unconformity are normally compacted. However, if the thickness of eroded section associated with the unconformity exceeds the thickness of younger sediment above it, then the lithologies beneath the unconformity will be over-compacted. The consequence of such over-compaction would be that the subsidence of the Miocene Unconformity, detailed above, is a lower bound.

5. Discussion

5.1. Potential causes of Miocene subsidence

Subsidence analysis using 3D flexural backstripping indicates that the south-western part of the Valencia Trough has subsided by at least 1.5 km on average since the formation of the Miocene Unconformity at sea level (Fig. 8). Based on this, we estimate a minimum subsidence rate of at least 90 m/Myr averaged over 17 Myr. We examine mechanisms for this rapid large amplitude subsidence, including: (i) Cenozoic and/or Mesozoic rifting, (ii) flexural loading from the Betic fold and thrust belt, (iii) subduction retro-arc dynamic subsidence and (iv) subduction back-arc (i.e. retro-arc) uplift followed by collapse.

(*i*) *Cenozoic and/or Mesozoic rifting*

One mechanism considered is subsidence due to rifting. Rifting in the Valencia Trough occurred in the Upper Triassic, Early Cretaceous and Cenozoic (Fig. 2).

Early Neogene subsidence and extensional faulting is observed in the north-eastern Valencia Trough and is interpreted as the consequence of the late Oligocene to early Miocene rifting preceding the opening of the nearby Liguro-Provençal Basin (Fig. 1 and 9, e.g., Watts and Torné, 1992b; Roca and Desegaulx, 1992). However, in our study area in the south-west of the Valencia Trough no significant Cenozoic extensional faults are observed either before or subsequent to the Miocene Unconformity (Fig. 4, 5 and 6). Most of the identified extensional faults show limited displacements and are located to the west in eastern Iberia (Roca et al., 2006) and to the east in the Balearic promontory (Etheve et al., 2016). In our area, the observed extensional faults are younger (late Miocene to Pliocene) and sole out on the Upper Triassic evaporite sequence (SU E) (Fig. 5 and 7d) with no clear counterpart in the underlying basement.

Cretaceous extensional faults are observed and formed during the latest Jurassic to Early Cretaceous rifting that locally thinned the crust under the Columbrets Basin (Fig. 4 and 5, Etheve et al., 2018). The magnitude of the Triassic rifting is unknown. We estimate that remaining Mesozoic post-rift thermal subsidence would be no more than 200 m assuming McKenzie (1978). All observations indicate that in the south-western Valencia Trough the 1.5 km of subsidence of the Miocene Unconformity is neither explained by Cenozoic or earlier Mesozoic rifting.

(*ii*) *Flexural loading from Betic thrusting*

Another potential cause of subsidence of the Miocene Unconformity could be from Betic thrust sheet loading. Large values of subsidence between 2-2.5 km are observed directly north of the mapped Betic front (Fig. 8) where Miocene sediments of SU B are up to 2-2.5 km thick (Fig. 7b) suggesting the formation of a narrow Miocene flexural foredeep basin at this location. This interpretation is consistent with the observed onlap architecture of the sediments (Fig. 6). South of the Betic front, thick depocentres of Miocene sediments show ellipsoid patterns (Fig. 7b) and correspond to subsidence since the Miocene Unconformity of 1.5 to 2.5 km. The observed pattern of these depocentres suggests they are controlled by the salt (Fig. 6 and 7e). The depocentres observed south of the Betic front are located between reactivated salt structures and are likely formed during the migration of the thin skin fold and thrust belt (Duffy et al., 2018). This interpretation is consistent with the observed numerous unconformities suggesting a migration of contractional deformation largely controlled by salt mobility (Fig. 6). North and west of the Betic fold and thrust belt, flexure resulting from thrust sheet loading can explain the large values of subsidence determined directly north of the Betic front (2-2.5 km). However, thin-skin deformation combined with the absence of significant topographies directly to the south and to the east is unlikely to produce sufficient loading effects to explain, alone, the average 1.5 km of subsidence of the Miocene Unconformity (Fig. 8f) in the south-western Valencia Trough.

(*iii*) *Subduction dynamic subsidence*

Another mechanism suggested to explain the Cenozoic subsidence of Western Mediterranean basins is subduction dynamic subsidence as shown by Do Couto et al. (2016) for the Alboran Basin located over the westward retreating slab of the Gilbraltar-Betic arc. Subduction dynamic subsidence (negative dynamic topography) is generated by the positive mass anomaly of the subducting slab in the mantle (Mitrovica et al., 1989; Gurnis, 1993). In the retro-arc (back-arc) region this subsidence has a long wavelength exceeding 1000 km in lateral extent with amplitude between 1 and 2 km (Mitrovica et al., 1989; Gurnis, 1993). During the Oligocene the Valencia Trough was located in the retroarc (back-arc) of Western Mediterranean subduction (Roca, 2001; Faccenna et al., 2004; Romagny et al., 2020) and would have experienced subduction retro-arc (back-arc) dynamic subsidence. However, since then, through the Miocene, subduction has propagated westwards and southwards (Faccenna et al., 2004; Van Hinsbergen et al., 2014; Romagny et al., 2020) and has slowed or ceased under the Valencia Trough which would have resulted in relative uplift rather than subsidence (as subduction dynamic subsidence diminished). In contrast to the Alboran Basin, subduction dynamic subsidence cannot be responsible for the rapid subsidence of the Valencia Trough since the Miocene Unconformity.

(*iv*) *Collapse and thermal equilibration of subduction back-arc uplift*

Our preferred explanation for the rapid and large amplitude subsidence of the Miocene Unconformity is the collapse of subduction related back-arc (retro-arc) uplift generated by subduction slab tear, associated with erosion. Onset of the Tethyan subduction slab roll-back in the late Oligocene is complex and 3D (Fig. 9a) with eastwards, southwards and westwards retreat of the subduction zone accommodated by subduction segmentation, slab tear and lithosphere delamination (Faccenna et al., 2004; Van Hinsbergen et al., 2014; Jolivet et al., 2021). Plate kinematic reconstructions suggest that subduction segmentation started in the Oligocene at the south-eastward prolongation of the North Balearic Transfer Zone (Fig. 9a, Van Hinsbergen et al., 2014). Subduction segmentation during rollback resulted in slab tear and would have triggered an upward flow of asthenosphere through the slab tear window in the back-arc asthenosphere wedge (Van Hinsbergen et al., 2014). The replacement of cool back-arc asthenosphere wedge by normal temperature asthenosphere together with heating or delamination of the lower continental lithosphere under the Valencia Trough would have generated uplift as the isostatic response. Because the Valencia Trough was at or near sea level in the late Paleogene, uplift would have resulted in subaerial erosion forming the Miocene Unconformity (Fig. 9a). Ther-

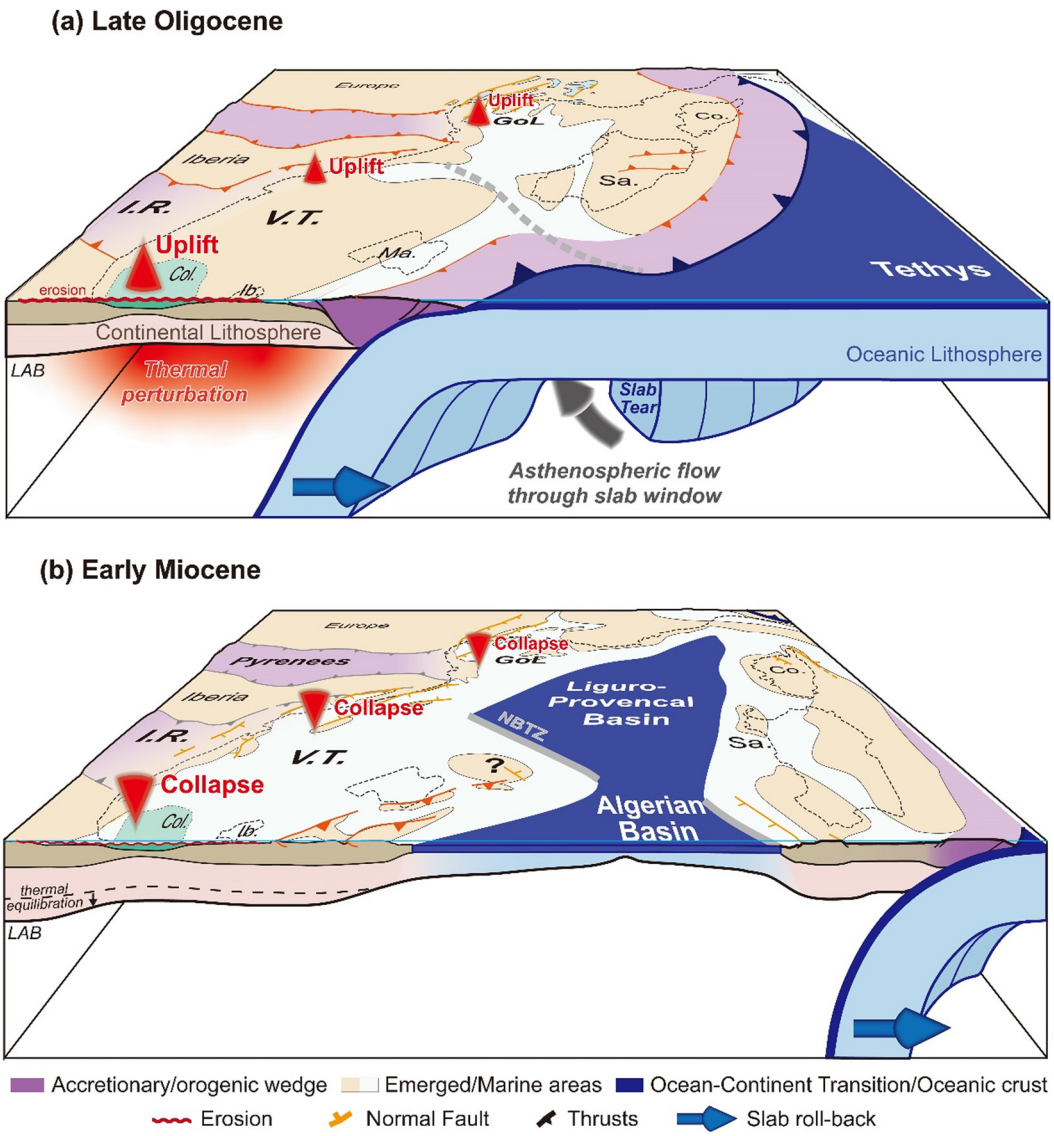

Fig. 9. 3D blocks illustrating the evolution of vertical movements in the Valencia Trough with respect to the 3D subduction slab dynamics during the Tethyan slab roll-back. (a) Late Oligocene: Subduction segmentation during roll-back resulting in slab tear would have generated an upward flow of asthenosphere through the slab tear window in back-arc asthenosphere wedge generating a thermal perturbation, transient uplift and erosion in the south-western Valencia Trough. (b) Early Miocene: collapse of transient uplift and thermal re-equilibration of the lithosphere caused the rapid subsidence of the Miocene Unconformity during the retreat of the Tethyan subduction. Paleogeographic maps are modified from Roca (2001) and Etheve et al. (2016). COT: Continent-Ocean-Transition. Be: Betics; Co.: Corsica; GoL: Gulf of Lion; I.R.: Iberian Range; NBTZ: North Balearic Transfer Zone; Sa.: Sardinia; V.T.: Valencia Trough.

mal re-equilibration of the thinned lower continental lithosphere under the Valencia Trough alone cannot account for the 1.5 km of subsidence of the Miocene Unconformity; the lack of any significant Cenozoic extensional faulting rules out whole lithosphere thermal re-equilibration subsidence. This suggests that part of the back-arc uplift may have been dynamically supported by mantle flow; the removal of that support contributing, together with thermal re-equilibration, to the observed rapid subsidence. The collapse of transient uplift resulting in the rapid subsidence of the Miocene Unconformity in the Valencia Trough correlates with rapid westward and southward migration of subduction slab roll-back (Fig. 9b, Faccenna et al., 2004; Van Hinsbergen et al., 2014; Romagny et al., 2020).

5.2. Estimations of the amount of erosion

Field, seismic and drill core observations all indicate that the Miocene unconformity results from an intense erosion, however, the amount of eroded material is to date unknown. Histograms of the subsidence to the Miocene Unconformity (Fig. 8) peak at just less than 1.5 km subsidence for Te $\geq$ 3. We use this subsidence measurement to estimate the amount of erosion, assuming that the uplift and collapse are of the same amplitude.

We have calculated erosion for different initial elevations and initial sediment thicknesses. To each different initial setting, we applied the same sequence of events: an uplift of 1.5 km, erosion to sea level and subsidence of 1.5 km (Fig. 10a). The 1.5 km magnitudes of uplift and subsidence are for water-loaded isostatic response; for the isostatic response above sea-level, the air-loaded equivalent (approximately 2/3 of the water-loaded magnitude) is used.

The remaining sediment thickness after uplift and erosion is plotted as a function of the initial elevation and sediment thickness (Fig. 10b). Based on the observed remaining sediment thickness in the Columbrets Basin (~8 km), we deduce that the initial sediment thickness was up to 12 km thick in the main Mesozoic depocentre before erosion. These values are consistent with those observed in basins formed during the same rifting phase, such as the Paren-

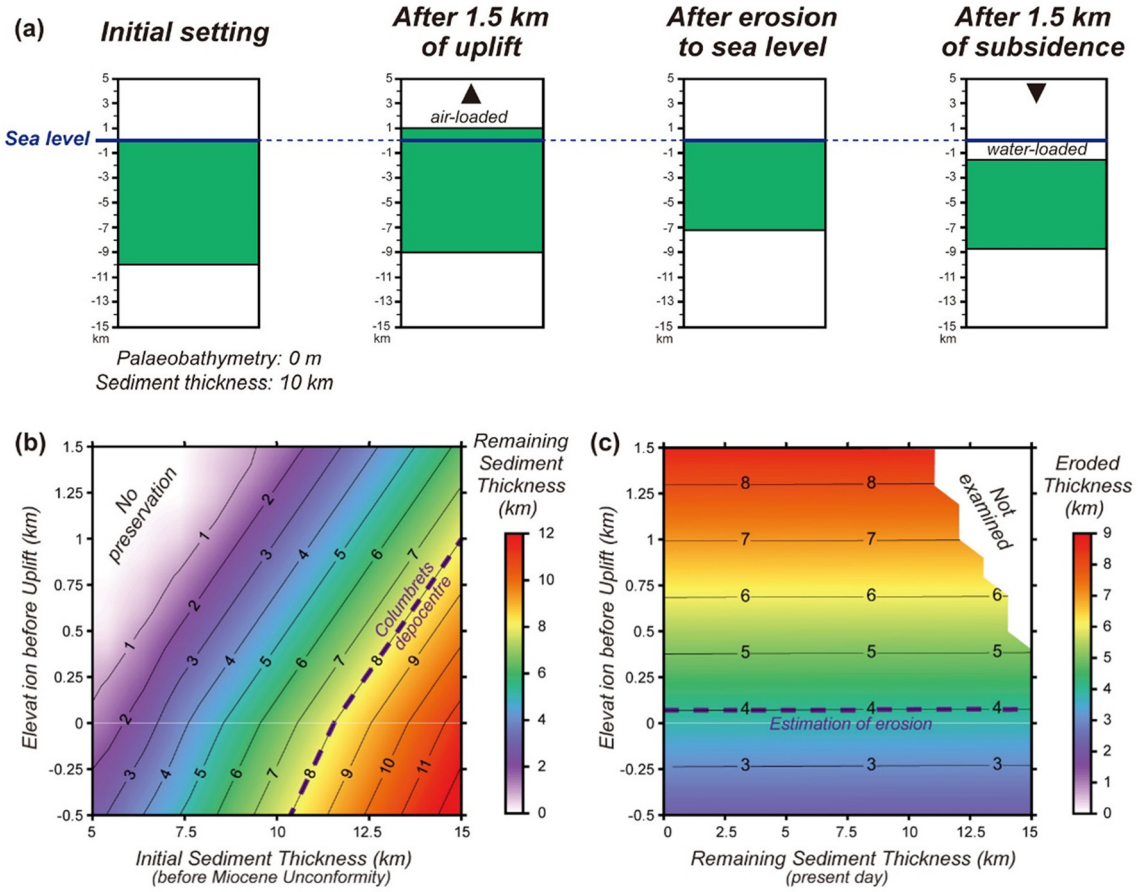

Fig. 10. (a) Sequence of events integrated in the flexural backstripping for different initial elevations and sediment thicknesses. (b) Plot of the remaining sediment thickness as a function of the initial elevation and sediment thickness. The observed remaining sediment thickness in the main Columbrets depocentre is indicated in purple (~ 8 km). (c) Plot of eroded thickness as a function of the initial elevation and remaining sediment thickness. (For interpretation of the colours in the figure(s), the reader is referred to the web version of this article.)

tis Basin located in the eastern Bay of Biscay (Fig. 1, Tugend et al., 2015a).

Based on these backstripping results we also deduce the theoretical thickness of eroded materials as a function of the initial elevation and remaining sediment thickness (Fig. 10c). Though uncertainties remain on the initial Palaeogene palaeobathymetry in our study area in the absence of Palaeogene sequences in the investigated wells, indirect observations suggest that the area was near sea level or locally emergent. Palaeogene sequences observed further to the north were deposited in subaerial to shallow marine environments (Roca et al., 1999). Based on these palaeobathymetric indications, we deduce from Fig. 10c that at least 4 km of erosion occurred in the south-western Valencia Trough. This estimation is consistent with the 5 km of Paleogene erosion interpreted from vitrinite reflectance data by Fernandez et al. (1995). Northwestward, in the adjacent Catalan Costal Range (Fig. 1) more than 2 km to 2.5 km of erosion are deduced for the Oligocene-Neogene from thermo-chronological results (Gaspar-Escribano et al., 2004; Ter Voorde et al., 2007).

The above erosion estimates assume that the magnitude of the transient uplift driving the erosion is equal to the measured 1.5 km subsidence of the Miocene Unconformity. As discussed earlier we believe that uplift was caused by thermal perturbations in the lithosphere and asthenosphere combined with mantle flow dynamic uplift. If this is the case, then some thermal re-equilibration and subsidence remains to occur indicating that the transient uplift would have exceeded 1.5 km and 4 km of erosion is an underestimate.

5.3. Integration of transient uplift in the Western Mediterranean geodynamics

Our investigation shows that the Miocene Unconformity formed above sea level during a regional uplift event and resulted in nearly 4 km of erosion. A series of unconformities formed prior to the Miocene are observed in the north-eastern part of the Valencia Trough (e.g., Maillard et al., 1992; Roca, 1996; Etheve et al., 2018; Roma et al., 2018) and as far north as in the Gulf of Lion (e.g., Gorini et al., 1993; Bache et al., 2010; Jolivet et al., 2015) and are commonly interpreted as being formed during the Oligo-Miocene rifting generated by the subduction slab roll back.

In the late Paleogene, at the future location of the Western Mediterranean, subduction of the Tethyan oceanic lithosphere was occurring under Eastern Iberia (Fig. 9a, Faccenna et al., 2004; Van Hinsbergen et al., 2014; Romagny et al., 2020). At the same time, Iberia was affected by convergence resulting in lithosphere thickening and tectonic uplift during the building of the Iberian Range and Pyrenean intra-continental mountain belts (Fig. 9a, Guimerà Rosso, 2018; Tugend et al., 2015b). Onset of the Tethyan subduction roll-back in the Oligocene generated a fundamental change in subduction dynamics resulting in the formation of the Gulf of Lion passive margin and oceanic Liguro-Provençal Basin (Fig. 9a, e.g., Romagny et al., 2020; Faccenna et al., 2004; Van Hinsbergen et al., 2014).

We note however the atypical subsidence evolution during the Oligocene-earliest Miocene rifting of the Gulf of Lion (Steckler and Watts, 1980; Bache et al., 2010; Jolivet et al., 2015). Rifting ini-

tiated under sub-aerial conditions associated with slow rates of subsidence, followed by a rapid early to middle Miocene phase of subsidence (Bache et al., 2010). Such atypical subsidence during rifting could indicate that the same pre-Miocene uplift event that we propose for the Valencia Trough might also have occurred in the Gulf of Lion to the north. Deep-seated mantle flow processes during the rifting of the Gulf of Lion have previously been inferred to explain its anomalous subsidence evolution (Steckler and Watts, 1980; Jolivet et al., 2015). A large part of the back-arc region seems to record a pre-Miocene uplift, supporting the idea that the uplift was generated by subduction segmentation and slab tear during roll-back. This uplift could be generated by a thermal event affecting back-arc lithosphere and asthenosphere, or mantle flow dynamic topography. While it is observationally difficult to discriminate between these (Molnar et al., 2015), we believe that the rapid subsidence of the Miocene Unconformity in the Valencia Trough is best explained by a combination of lithosphere thermal re-equilibration and the collapse of mantle dynamic uplift.

6. Conclusions

We have investigated the Cenozoic subsidence evolution of the south-western part of the Valencia Trough and show using 3D flexural backstripping subsidence analysis that the subaerially formed Miocene Unconformity observed in the south-western part of the Valencia Trough has subsided by 1.5 km on average since its formation. The limited occurrence of Cenozoic extensional faults indicates that Cenozoic rifting cannot explain the subsidence of the Miocene Unconformity. Neither can post-rift subsidence from earlier Mesozoic rifting. Flexural loading related to the Betic fold and thrust belt most likely controlled the local ($\sim$ 50 km wavelength) high subsidence values observed close to the deformation front but cannot explain the observed longer wavelength subsidence of the Miocene Unconformity in the Valencia Trough.

Instead, we propose that long-wavelength (> 500 km) rapid subsidence of the Miocene Unconformity was caused by the collapse of transient uplift generated by subduction segmentation and slab tear during the westward roll-back of Tethyan oceanic lithosphere subduction.

Our analysis suggests that the regional uplift leading to the Miocene Unconformity resulted in approximately 4 km of material being eroded. We propose that rapid km-scale back-arc uplift and subsidence may be a common occurrence globally for other back-arc regions experiencing subduction segmentation and slab-tear during subduction slab roll-back.

CRediT authorship contribution statement

Penggao Fang: Formal analysis, Investigation, Visualization, Writing – original draft, Writing – review & editing. **Julie Tugend:** Conceptualization, Formal analysis, Investigation, Methodology, Supervision, Validation, Visualization, Writing – original draft, Writing – review & editing. **Geoffroy Mohn:** Conceptualization, Investigation, Methodology, Project administration, Resources, Supervision, Visualization, Writing – review & editing. **Nick Kusznir:** Conceptualization, Investigation, Methodology, Resources, Writing – review & editing. **WeiWei Ding:** Funding acquisition, Supervision.

Declaration of competing interest

The authors declare that they have no known competing financial interests or personal relationships that could have appeared to influence the work reported in this paper.

Acknowledgements

The authors thank Sierd Cloetingh and Laurent Jolivet for their insightful reviews and Hans Thybo for his careful editorial handling. P. Fang and W. Ding acknowledge funding from the National Natural Science Foundation of China (Grant Nos. 42025601, 91858214). J. Tugend acknowledges the Orogen project and funding from TOTAL SA for her post-doctoral fellowship. The Generic Mapping Tools (GMT) and QGIS software were used in this work. Global topographic grid was extracted from the website of the UCSD (https://topex.ucsd.edu/WWW_html/srtm30_plus.html). Seismic data are available upon request at the Archivo Nacional de Hidrocarburos del Ministerio de Energía, Turismo y Agenda Digital de España (https://geoportal.minetur.gob.es/ATHv2/welcome.do).

Appendix A. Supplementary material

Supplementary material related to this article can be found online at https://doi.org/10.1016/j.epsl.2021.117179.

References

Alba, J.S., 2007. La Mancha Triassic and lower Lias stratigraphy, a well log interpretation. J. Iber. Geol. 33 (1), 55–78.

Arche, A., López Gómez, J., 1996. Origin of the Permian-Triassic Iberian basin, central-eastern Spain. Tectonophysics 266, 443–464. https://doi.org/10.1016/s0040-1951(96)00202-8.

Ayala, C., Torne, M., Roca, R., 2015. A review of the current knowledge of the crustal and lithospheric structure of the Valencia Trough Basin. Bol. Geol. Min. 126 (2–3), 533–552.

Bache, F., Olivet, J.L., Gorini, C., Aslanian, D., Labails, C., Rabineau, M., 2010. Evolution of rifted continental margins: the case of the Gulf of Lions (Western Mediterranean Basin). Earth Planet. Sci. Lett. 292 (3–4), 345–356. https://doi.org/10.1016/j.epsl.2010.02.001.

Cameselle, A.L., Urgeles, R., 2017. Large-scale margin collapse during Messinian early sea-level drawdown: the SW Valencia trough, NW Mediterranean. Basin Res. 29, 576–595. https://doi.org/10.1111/bre.12170.

Do Couto, D., Gorini, C., Jolivet, L., Lebret, N., Augier, R., Gumiaux , C., et al., 2016. Tectonic and stratigraphic evolution of the Western Alboran Sea Basin in the last 25 Myrs. Tectonophysics 677, 280–311. https://doi.org/10.1016/j.tecto.2016.03.020.

Duffy, O.B., Dooley, T.P., Hudec, M.R., Jackson, M.P., Fernandez, N., Jackson, C.A., Soto, J.I., 2018. Structural evolution of salt-influenced fold-and-thrust belts: a synthesis and new insights from basins containing isolated salt diapirs. J. Struct. Geol. 114, 206–221. https://doi.org/10.31223/osf.io/nd7et.

Etheve, N., Frizon de Lamotte, D., Mohn, G., Martos, R., Roca, E., Blanpied, C., 2016. Extensional vs contractional Cenozoic deformation in Ibiza (Balearic Promontory, Spain): integration in the West Mediterranean back-arc setting. Tectonophysics 682, 35–55. https://doi.org/10.1016/j.tecto.2016.05.037.

Etheve, N., Mohn, G., Frizon de Lamotte, D., Roca, E., Tugend, J., Gómez-Romeu, J., 2018. Extreme Mesozoic crustal thinning in the eastern Iberia margin: the example of the Columbrets Basin (Valencia Trough). Tectonics 37 (2), 636–662. https://doi.org/10.1002/2017tc004613.

Faccenna, C., Piromallo, C., Crespo-Blanc, A., Jolivet, L., Rossetti, F., 2004. Lateral slab deformation and the origin of the western Mediterranean arcs. Tectonics 23 (1). https://doi.org/10.1029/2002tc001488.

Fernandez, M., Foucher, J.P., Jurado, M.J., 1995. Evidence for the multi-stage formation of the south-western Valencia Trough. Mar. Pet. Geol. 12 (1), 101–109. https://doi.org/10.1016/0264-8172(95)90390-6.

Fontboté, J.M., Guimerà, J., Roca, E., Sàbat, F., Santanach, P., Fernández-Ortigosa, F., 1990. The Cenozoic geodynamic evolution of the Valencia trough (western Mediterranean). Rev. Soc. Geol. Esp. 3 (3–4), 249–259.

Gaspar-Escribano, J.M., Garcia-Castellanos, D., Roca, E., Cloetingh, S.A.P.L., 2004. Cenozoic vertical motions of the Catalan Coastal Ranges (NE Spain): the role of tectonics, isostasy, and surface transport. Tectonics 23 (1). https://doi.org/10.1029/2003tc001511.

Gaspar-Escribano, J.M., Ter Voorde, M., Roca, E., Cloetingh, S.A.P.L., 2003. Mechanical (de-) coupling of the lithosphere in the Valencia Trough (NW Mediterranean): what does it mean? Earth Planet. Sci. Lett. 210 (1–2), 291–303. https://doi.org/10.1016/s0012-821x(03)00140-7.

Gaspar-Escribano, J.M., Van Wees, J.D., Ter Voorde, M., Cloetingh, S.A.P.L., Roca, E., Cabrera, L., et al., 2001. Three-dimensional flexural modelling of the Ebro Basin (NE Iberia). Geophys. J. Int. 145 (2), 349–367. https://doi.org/10.1046/j.1365-246x.2001.01379.x.

Gorini, C., Le Marrec, A., Mauffret, A., 1993. Contribution to the structural and sedimentary history of the Gulf of Lions (western Mediterranean) from the ECORS profiles, industrial seismic profiles and well data. Bull. Soc. Géol. Fr. 164 (3), 353–363.

Granado, P., Urgeles, R., Sàbat, F., Albert-Villanueva, E., Roca, E., Muñoz, J.A., Mazzuca, N., Gambini, R., 2016. Geodynamical framework and hydrocarbon plays of a salt giant: the NW Mediterranean Basin. Pet. Geosci. 22 (4), 309–321. https://doi.org/10.1144/petgeo2015-084.

Guimerà Rosso, J.J., 2018. Structure of an intraplate fold-and-thrust belt: the Iberian Chain. A synthesis. Geol. Acta 16 (4), 0427.

Gurnis, M., 1993. Phanerozoic marine inundation of continents driven by dynamic topography above subducting slabs. Nature 364 (6438), 589–593.

Janssen, M.E., Torné, M., Cloetingh, S.A.P.L., Banda, E., 1993. Pliocene uplift of the eastern Iberian margin: inferences from quantitative modelling of the Valencia Trough. Earth Planet. Sci. Lett. 119 (4), 585–597. https://doi.org/10.1016/0012-821x(93)90064-g.

Jolivet, L., Gorini, C., Smit, J., Leroy, S., 2015. Continental breakup and the dynamics of rifting in back-arc basins: the Gulf of Lion margin. Tectonics 34 (4), 662–679. https://doi.org/10.1002/2014TC003570.

Jolivet, L., Menant, A., Roche, V., Le Pourhiet, L., Maillard, A., Augier, R., Do Couto, D., Gorini, C., Thinon, I., Canva, A., 2021. Transfer zones in Mediterranean back-arc regions and tear faults. In: Lacombe, O., Tavani, S., Teixell, A., Pedreira, D., Calassou, S. (Eds.), BSGF - Earth Sciences Bulletin 192 (1), 11. https://doi.org/10.1051/bsgf/2021006.

Klimowitz, J., Escalante, S., Hernández, E., Soto, J.I., 2018. Estructuración tectónica Alpina del margen occidental del Surco de Valencia (Mediterráneo Occidental). Rev. Soc. Geol. Esp. 31 (2), 83–100.

Lanaja, J.M., 1987. Contribución de la exploración petrolífera al conocimiento de la geología de España. IGME.

Maillard, A., Gorini, C., Mauffret, A., Sage, F., Lofi, J., Gaullier, V., 2006. Offshore evidence of polyphase erosion in the Valencia Basin (Northwestern Mediterranean): scenario for the Messinian Salinity Crisis. Sediment. Geol. 188, 69–91. https://doi.org/10.1016/j.sedgeo.2006.02.006.

Maillard, A., Mauffret, A., 1999. Crustal structure and riftogenesis of the Valencia Trough (north-western Mediterranean Sea). Basin Res. 11 (4), 357–379. https://doi.org/10.1046/j.1365-2117.1999.00105.x.

Maillard, A., Mauffret, A., 2013. Structure and present-day compression in the offshore area between Alicante and Ibiza Island (Eastern Iberian Margin). Tectonophysics 591, 116–130. https://doi.org/10.1016/j.tecto.2011.07.007.

Maillard, A., Mauffret, A., Watts, A.B., Torné, M., Pascal, G., Buhl, P., Pinet, B., 1992. Tertiary sedimentary history and structure of the Valencia trough (western Mediterranean). Tectonophysics 203 (1–4), 57–75. https://doi.org/10.1016/0040-1951(92)90215-r.

McKenzie, D., 1978. Some remarks on the development of sedimentary basins. Earth Planet. Sci. Lett. 40 (1), 25–32.

Mitrovica, J.X., Beaumont, C., Jarvis, G.T., 1989. Tilting of continental interiors by the dynamical effects of subduction. Tectonics 8, 1079–1094.

Molnar, P., England, P.C., Jones, C.H., 2015. Mantle dynamics, isostasy, and the support of high terrain. J. Geophys. Res., Solid Earth 120 (3), 1932–1957. https://doi.org/10.1002/2014jb011724.

Ortí, F., Pérez-López, A., Salvany, J.M., 2017. Triassic evaporites of Iberia: sedimentological and palaeogeographical implications for the western Neotethys evolution during the Middle Triassic–Earliest Jurassic. Palaeogeogr. Palaeoclimatol. Palaeoecol. 471, 157–180. https://doi.org/10.1016/j.palaeo.2017.01.025.

Pascal, G., Torné, M., Buhl, P., Watts, A.B., Mauffret, A., 1992. Crustal and velocity structure of the Valencia trough (western Mediterranean), Part II. Detailed interpretation of five Expanded Spread Profiles. Tectonophysics 203 (1–4), 21–35. https://doi.org/10.1016/0040-1951(92)90213-p.

Platt, J.P., Behr, W.M., Johanesen, K., Williams, J.R., 2013. The Betic-Rif arc and its orogenic hinterland: a review. Annu. Rev. Earth Planet. Sci. 41, 313–357. https://doi.org/10.1146/annurev-earth-050212-123951.

Roberts, A.M., Kusznir, N.J., Yielding, G., Styles, P., 1998. Backstripping extensional basins: the need for a sideways glance. Pet. Geosci. 4, 327–338.

Roca, E., 1996. La cubeta mesozoica de las Columbrets: aportaciones al conocimiento de la estructura del surco de Valencia. Geogaceta 20 (7), 1711–1714.

Roca, E., 2001. The northwest Mediterranean basin (Valencia trough, Gulf of Lions and Liguro-Provencal basins): structure and geodynamic evolution. Mém. Mus. Natl. Hist. Nat. (1993) 186, 671–706.

Roca, E., Desegaulx, P., 1992. Analysis of the geological evolution and vertical movements in the Valencia Trough area, western Mediterranean. Mar. Pet. Geol. 9 (2), 167–185. https://doi.org/10.1016/0264-8172(92)90089-w.

Roca, E., Guimerà, J., 1992. The Neogene structure of the eastern Iberian margin: structural constraints on the crustal evolution of the Valencia trough (western Mediterranean). Tectonophysics 203 (1–4), 203–218. https://doi.org/10.1016/0040-1951(92)90224-t.

Roca, E., Sans, M., Cabrera, L., Marzo, M., 1999. Oligocene to Middle Miocene evolution of the central Catalan margin (northwestern Mediterranean). Tectonophysics 315 (1–4), 209–229. https://doi.org/10.1016/s0040-1951(99)00289-9.

Roca, E., Sans, M., Koyi, H.A., 2006. Polyphase deformation of diapiric areas in models and in the eastern Prebetics (Spain). AAPG Bull. 90 (1), 115–136. https://doi.org/10.1306/07260504096.

Roma, M., Ferrer, O., Roca, E., Pla, O., Escosa, F.O., Butillé, M., 2018. Formation and inversion of salt-detached ramp-syncline basins. Results from analog modeling and application to the Columbrets Basin (Western Mediterranean). Tectonophysics 745, 214–228. https://doi.org/10.1016/j.tecto.2018.08.012.

Romagny, A., Jolivet, L., Menant, A., Bessière, E., Maillard, A., Canva, A., Gorini, C., Augier, R., 2020. Detailed tectonic reconstructions of the Western Mediterranean region for the last 35 Ma, insights on driving mechanisms. In: Lacombe, O., Tavani, S., Teixell, A., Pedreira, D., Calassou, S. (Eds.), BSGF - Earth Sciences Bulletin 191 (1), 37. https://doi.org/10.1051/bsgf/2020040.

Sàbat, F., Gelabert, B., Rodríguez-Perea, A., Giménez, J., 2011. Geological structure and evolution of Majorca: implications for the origin of the Western Mediterranean. Tectonophysics 510 (1–2), 217–238. https://doi.org/10.1016/j.tecto.2011.07.005.

Sàbat, F., Roca, E., Muñoz, J.A., Vergés, J., Santanach, P., Sans, M., Masana, E., Estévez, A., Santisteban, C., 1997. Role of extension and compression in the evolution of the eastern margin of Iberia: the ESCI-València Trough seismic profile. Rev. Soc. Geol. Esp. 8, 431–448.

Salas, R., Guimerà, J., Mas, R., Martín-Closas, C., Meléndez, A., Alonso, A., 2001. Evolution of the Mesozoic central Iberian Rift system and its Cainozoic inversion (Iberian chain). Peri-Tethys Memoir 6, 145–185.

Sclater, J.G., Christie, P.A., 1980. Continental stretching: an explanation of the post-mid-Cretaceous subsidence of the central North Sea basin. J. Geophys. Res., Solid Earth 85 (B7), 3711–3739. https://doi.org/10.1306/2f919201-16ce-11d7-8645000102c1865d.

Steckler, M.S., Watts, A.B., 1980. The Gulf of Lion: subsidence of a young continental margin. Nature 287 (5781), 425–429.

Ter Voorde, M., Gaspar-Escribano, J.M., Juez-Larré, J., Roca, E., Cloetingh, S.A.P.L., Andriessen, P., 2007. Thermal effects of linked lithospheric and upper crustal–scale processes: insights from numerical modeling of the Cenozoic Central Catalan Coastal Ranges (NE Spain). Tectonics 26 (5).

Torné, M., Pascal, G., Buhl, P., Watts, A.B., Mauffret, A., 1992. Crustal and velocity structure of the Valencia trough (western Mediterranean), Part I. A combined refraction/wide-angle reflection and near-vertical reflection study. Tectonophysics 203 (1–4), 1–20. https://doi.org/10.1016/0040-1951(92)90212-o.

Torres, J., Bois, C., Burrus, J., 1993. Initiation and evolution of the Valencia Trough (western Mediterranean): constraints from deep seismic profiling and subsidence analysis. Tectonophysics 228 (1–2), 57–80. https://doi.org/10.1016/0040-1951(93)90214-5.

Tugend, J., Manatschal, G., Kusznir, N.J., Masini, E., 2015a. Characterizing and identifying structural domains at rifted continental margins: application to the Bay of Biscay margins and its Western Pyrenean fossil remnants. Geol. Soc. (Lond.) Spec. Publ. 413 (1), 171–203. https://doi.org/10.1144/sp413.3.

Tugend, J., Manatschal, G., Kusznir, N.J., 2015b. Spatial and temporal evolution of hyperextended rift systems: implication for the nature, kinematics, and timing of the Iberian-European plate boundary. Geology 43 (1), 15–18. https://doi.org/10.1130/g36072.1.

Van der Beek, P.A., Cloetingh, S., 1992. Lithospheric flexure and the tectonic evolution of the Betic Cordilleras (SE Spain). Tectonophysics 203 (1–4), 325–344. https://doi.org/10.1016/0040-1951(92)90230-4.

Van Hinsbergen, D.J., Vissers, R.L., Spakman, W., 2014. Origin and consequences of western Mediterranean subduction, rollback, and slab segmentation. Tectonics 33 (4), 393–419. https://doi.org/10.1002/2013tc003349.

Watts, A.B., Torné, M., 1992a. Crustal structure and the mechanical properties of extended continental lithosphere in the Valencia trough (western Mediterranean). J. Geol. Soc. 149 (5), 813–827. https://doi.org/10.1144/gsjgs.149.5.0813.

Watts, A.B., Torné, M., 1992b. Subsidence history, crustal structure, and thermal evolution of the Valencia Trough: a young extensional basin in the western Mediterranean. J. Geophys. Res., Solid Earth 97 (B13), 20021–20041. https://doi.org/10.1029/92jb00583.

Yamasaki, T., Stephenson, R., 2009. Change in tectonic force inferred from basin subsidence: implications for the dynamical aspects of back-arc rifting in the western Mediterranean. Earth Planet. Sci. Lett. 277 (1–2), 174–183. https://doi.org/10.1016/j.epsl.2008.10.011.